Toxicology 259 (2009) 140–148

Contents lists available at ScienceDirect

Toxicology

journal homepage: www.elsevier.com/locate/toxicol

# Retrospective analysis of 4-week inhalation studies in rats with focus on fate and pulmonary toxicity of two nanosized aluminum oxyhydroxides (boehmite) and pigment-grade iron oxide (magnetite): The key metric of dose is particle mass and not particle surface area

Jürgen Pauluhn*

*Institute of Toxicology, Bayer Schering Pharma, Department of Inhalation Toxicology, Building no. 514, 42096 Wuppertal, Germany*

ARTICLE INFO

*Article history:*
Received 19 January 2009
Received in revised form 14 February 2009
Accepted 21 February 2009
Available online 5 March 2009

*Keywords:*
Nanoparticles
Repeated inhalation exposure
Disposition
Respirability
Clearance
Aggregates
Dose metric
Pulmonary toxicity
Dosimetry

ABSTRACT

This paper compares the pulmonary toxicokinetics and toxicodynamics of three different types of poorly soluble dusts examined in repeated rat inhalation bioassays (6 h/day, 5 days/week, 4 weeks). In these studies the fate of particles was studied during a 3–6-month postexposure period. This retrospective analysis included two types of aluminum oxyhydroxides (AlOOH, boehmite), high purity calcined, and agglomerated nanosized aluminas of very low solubility with primary isometric particles of 10 or 40 nm, and synthetic iron oxide black ($Fe_3O_4$ pigment grade). Three metrics of dose (actual mass concentration, surface area concentration, mass-based lung burden) were compared with pulmonary toxicity characterized by bronchoalveolar lavage. The results of this analysis provide strong evidence that pulmonary toxicity (inflammation) corresponds best with the mass-based cumulative lung exposure dose. The inhalation study with a MMAD of ≈0.5 μm yielded a higher pulmonary dose than MMADs in the range of 1–2 μm, a range most commonly used in repeated exposure inhalation studies. Hence, a key premise for the dosimetric adjustment across species is that comparable lung tissue doses should cause comparable effects. From that perspective, the determination of mass-based pulmonary lung burdens appears to be amongst the most important and critical nominator of dose and dose-related pulmonary toxicity.



## 1. Introduction

Published evidence demonstrates that ultrafine $TiO_2$ particles caused more inflammation in rat lungs than exposure to fine $TiO_2$ (Ferin et al., 1992; Bermudez et al., 2002, 2004). These differences in toxic potencies seem to be a result of their unique size, surface area/activity and/or crystal properties (Warheit et al., 2005, 2007; Warheit, 2008). In rats, pulmonary inflammatory responses increase precipitously under conditions of lung overload, a particle-induced depression of clearance as a consequence of volumetric overload of the alveolar macrophages and associated loss of alveolar macrophage mobility (Monteiller et al., 2007; Morrow, 1988, 1992; Stöber and McClellan, 1997). Interestingly, the alveolar clearance rate of the human is thought to be independent of the particulate matter (PM) load for expected exposures, but the clearance rate for a rat depends on the amount of particles in the alveolar region. Hence, rats appear to be susceptible to "overload"-related effects due to impaired macrophage-mediated alveolar clearance (Brown et al., 2005).

Overload has been loosely defined as the alveolar burden causing a two- to four-times reduction in alveolar clearance rates relative to normal clearance rates (International Life Science Institute (ILSI), 2000). A unifying, most appropriate metric of poorly soluble particles conferring pulmonary biopersistence and toxicity is still controversially discussed. Accordingly, it is timely to analyse empirical data from inhalation studies in rats to consider as to which extent current testing paradigms are appropriate to identify the unique hazards potentially associated with nano-sized materials (smaller than 0.1 μm at least in one dimension) relative to pigment-sized, fine PMs. For pigments an optimal particle size exists with respect to lightening power and for a given particle size there is an optimal wavelength for maximum light scattering. Depending on the color, tinge, hue, and refractive index, this optimal particle size of many pigments is in the range of ≈0.1–1 μm (Ullmann, 1992).

The purpose of this paper is to retrospectively compare the pulmonary toxicokinetics and toxicodynamics of three different types of poorly soluble dusts examined in 4-week rat inhalation bioassays. The fate of particles was studied during a 3–6-month postexposure period. The substances addressed included two

* Tel.: +49 202 363909; fax: +49 202 364589.
*E-mail address:* juergen.pauluhn@bayerhealthcare.com.

0300-483X/$ – see front matter © 2009 Elsevier Ireland Ltd. All rights reserved.
doi:10.1016/j.tox.2009.02.012

types of aluminum oxyhydroxides (boehmite), high purity calcined, and agglomerated nanosized aluminas of very low solubility. These aluminas had primary isometric particles of 10 and 40 nm. The size of agglomerated particles in inhalation chambers was MMAD ≈1.7 and ≈0.6 μm, respectively. This size-range of primary particles was similar to that of ultrafine antase/rutile $TiO_2$ (average particle size ≈25 nm) examined by Bermudez et al. (2002, 2004). The particular advantage of using nanosized AlOOH is that different crystal structures with resultant differences in toxic potency due to dissimilarities in crystal properties (Warheit et al., 2007) are not expected to occur. These aluminas are free flowing high purity agglomerated powders with optimized properties augmenting their dispersion in various systems. They found their way into a broad range of applications, including catalyst supports, coatings, polymer additives, thickeners, refractories, abrasives, ceramics as well as flame retardant in plastics. Further details regarding their use and properties are available elsewhere (http://www.sasoltechdata.com/alumina_group.asp). Opposite to these materials, the high purity iron oxide black pigment (magnetite) has a larger size of crystals (300–600 nm). While the surface area of $Fe_3O_4$ was 10.5 $m^2/g$, that of AlOOH-10 nm was 182 $m^2/g$. Magnetite is produced by slow crystallization and decomposes at temperatures above 80 °C. Calcination of magnetite leads to red iron oxide (hematite, $Fe_2O_3$). The specific density of AlOOH and $Fe_3O_4$ is 2.9 and 4.7 $mg/cm^3$, respectively.

The volume of micron-sized, agglomerated arrangements of closely packed particles increase with lower specific density of particles. Hence, the composite volume of AlOOH agglomerates is higher than that of magnetite agglomerates. Consequently, much less particle mass would be needed for AlOOH to exceed the volumetric overload limit for the inhibition of macrophage-mediated clearance, which is estimated to start at ≈60 $\mu m^3$ per alveolar macrophage (Morrow, 1988) or at lung burdens of ≈1 mg particles/g lung or greater (Morrow, 1992). Loaded alveolar macrophages may be considered immobile at 10-times or thereabouts of volumetric loading. While the specific density of primary particles is commonly well defined, equivalent data for agglomerated particles are more difficult to define. This issue is further complicated due to the interrelationship of particle size-dependent changes in void-space volume and the specific density of primary particles.

At least hypothetically, synthetic iron pigments may be subject to enhanced dissolution in lung tissue due to the presence of iron-binding, chelating proteins. Free, i.e., non-chelated iron catalyzes autoxidations by Fenton and Haber–Weiss reactions, resulting in the production of reactive oxygen species (Bacon and Britton, 1990; Fubini et al., 1995; Winterbourn, 1995). Chelates may also participate in a coupled cellular protection mechanism in which iron storage protein, ferritin, ultimately provides protection by sequestering and oxidizing of free iron. Iron is transported to intracellular sites of reutilization and/or storage in ferritin or hemosiderin but this aspect of iron metabolism, including the elusive pool of "free", i.e., catalytically active iron and its cellular trafficking, remains enigmatic. These aspects were addressed by using an integrated approach, i.e., a comparison of the particle elimination kinetics from the lung and inflammogenic potency relative to AlOOH which cannot undergo redox-cycling.

Suffice it to say, this retrospective comparison requires a mass-based metric to have common denominators for inhalation exposure, particle size measurements, and analysis of lung burdens. However, additional attempts were made to link the actual 'target organ dose' and associated pulmonary inflammation to either PM-mass, -surface area or -lung burden. However, due to the difficulty to reliably estimate PM volumes from aggregated PMs with different densities, polydisperse particle sizes, and void-spaces of packed particles within macrophages, volumetric estimates, although considered to be mechanistically important (Brown et al., 2005; Morrow, 1988, 1992; Oberdörster et al., 1992), were not considered in this analysis.

**Table 1**
Physical characteristics of test substances.

| Test substance | Boehmite | Boehmite | Magnetite |
|---|---|---|---|
| Empirical formula | γ-AlO(OH) | γ-AlO(OH) | $Fe_3O_4$ |
| Commercial name | Pural® 200[a] | Disperal®[a] | Ferroxide® Black 88P[b] |
| Metal content (%) | 43.9 | 39.4 | 69.5 |
| $N_2$-BET surface area ($m^2/g$) | 105 | 182 | 10.5 |
| Specific density ($g/cm^3$) | 2.9 | 2.9 | 4.6–4.8 |
| Loose bulk density ($g/cm^3$) | 0.51 | 0.46 | 0.6–0.8 |
| Primary particle size (nm) | ≈40 | ≈10 | 300–600 |
| Micronization (due to low dustiness) | No | Yes | No |

Further details of these products are available under the producers' websites (http://www.sasoltechdata.com/alumina_group.asp; http://www.rockwoodpigments.com/Tech).

[a] High purity aluminas from Sasol, Hamburg, Germany.

[b] Pigment from Rockwood Italia, Torino, Italy.

## 2. Methods

### 2.1. Test material

High purity, calcined aluminum oxyhydroxides (empirical formula: γ-AlOOH, primary particle size 10 or 40 nm) and high purity synthetic crystallized black iron oxide (empirical formula: $Fe_3O_4$, primary particle size 300–600 nm). Their sources and physical properties are given in Table 1.

### 2.2. Animals, diet, and housing conditions

Specific-pathogen-free, young adult male Wistar rats of the strain Bor: WISW (SPF-Cpb) were from Winkelmann, Borchen, Germany. At the commencement of the study the rats were approximately 2 months old and were quarantined for approximately 1 week prior to being used. In all studies, at the commencement and end of the exposure periods rats weighed ≈230 and ≈280 g, respectively. They were singly housed in polycarbonate cages, containing low-dust wood shavings as bedding material. A standard fixed-formula diet (KLIBA 3883 = NAFAG 9441 pellets maintenance diet for rats and mice; PROVIMI KLIBA SA, 4303 Kaiseraugst, Switzerland) and municipality tap water (drinking bottles) were available *ad libitum*. The light cycle was automatically controlled in the animal room to provide 12/12 h light/darkness. Temperature and relative humidity were in the range of 22 °C and 40–60%, respectively. The studies described were conducted in accordance to the EU animal welfare regulations (European Community, Directive 86/609/EEC, 1986).

### 2.3. Test design

Exposure of groups of male rats was for 6 h/day, and 5 days/week for 4 consecutive weeks. At the end of the acclimatization period rats were randomly assigned to the exposure groups. The rats were exposed in directed-flow nose-only inhalation chambers and rats exposed under otherwise identical test conditions to dry, conditioned air served as concurrent control group. Postexposure periods ranged from 3 to 6 months. On each postexposure sacrifices 12 rats/group were used (six for lavage, six for toxicokinetic examinations). The focus of this analysis was on changes of inflammatory endpoints in lungs by bronchoalveolar lavage (BAL) approximately 1-week postexposure and dispositional pulmonary endpoints over the entire postexposure period to allow an estimation of the elimination kinetics of particles.

### 2.4. Exposure technique and atmosphere generation

In all three studies powders were dispersed into inhalation chambers using a Wright-Dust-Feeder (BGI Inc., Waltham, MA, USA). AlOOH-10 nm had a low dustiness. Therefore it was micronized to enhance the dustiness of the bulk material. For micronization a Retsch Centrifugal Ball Mill S100 was used. Prior to entering the nose-only inhalation chamber a cyclone and pull/push-dilution system were used to achieve the targeted particle size and concentration. Briefly, pressurized dry, clean air was used for powder dispersion. The flow rate per exposure port was 0.75 l/min. Further methodological details have been published in detail elsewhere (Pauluhn, 2009).

### 2.5. Exposure atmosphere characterization

In addition to continuous real-time monitoring of atmospheres, breathing zone concentrations were characterized by filter analyses (glass fiber filters, Sartorius,

Göttingen, Germany). Particle size analyses were made using a low-pressure critical orifice Berner-Type AERAS stainless steel 11-stage cascade impactor with effective cut-off diameters from 0.016 to 16 μm (HAUKE, Gmunden, Austria). Silicon-coated aluminum foil served as collection medium of particles. The mass median aerodynamic diameter (MMAD) and the geometric standard deviation (GSD) were calculated as described previously (Pauluhn, 2005).

*2.5.1. Bronchoalveolar lavage and lung weights*

After complete exsanguination by heart puncture, the excised wet lung was weighed and lavaged via a tracheal cannula. The lavage procedure used two lavage cycles each with a single volume of 5 ml/rat and cycle (20 ml/kg), provided a yield of $5.1 \pm 1.4 \times 10^6$ cells/g lung (air control, male Wistar rats). Similar yields ($4.8–5.7 \times 10^6$ cells/g lung) were reported using 12 lung washes (Brain and Frank, 1968a,b). This demonstrates that the lavage procedure applied collected the maximum technically number of cells. Hence, it appears to be technically demanding or not feasible to increase this yield of BAL-cells any further (Pauluhn, 2009).

*2.5.2. Particle disposition*

This analysis focused on the determination of metals in the lung as marker of exposure (for metal contents see Table 1). All data refer to the mass of metal oxide per lung. In the iron oxide study the right lung lobe was dissected for trace analysis. In the boehmite study metal contents were determined in both the lavaged lung and BAL-cells and the lung burden represents the sum of both. Organ aliquots were digested and converted to acid-soluble inorganic salts in a mixture of acids (e.g., nitric acid, hydrochloric acid, sulfuric acid, perchloric acid, and/or hydrogen peroxide). This conversion took place in sealed reaction vessels in a temperature range from 130 to 300 °C at 200 bar in a microwave-heated autoclave (Ultraclave MLS). After cooling, solubilized organs were diluted with deionized water. For all analyses blank solutions and a standard solution of the respective metal were used. The PerkinElmer AAnalyst™ 700 high-performance atomic absorption (AA) spectrometer with WinLab 32 AA software features was used for analysis of Al. The AA is an automated motorized atomizer exchange that allows switching between flame and graphite furnace AA by a simple software command. The graphite mode was used for determinations. The instrument was equipped with a high performance burner system and TotalFlow™ gas controls for flame AA and a Heated Graphite Atomizer (HGA®) graphite furnace with deuterium background corrector. The graphite furnace system includes true temperature control (TTC) and pyro tubes, providing full stabilized temperature platform furnace (STPF) conditions for almost interference-free trace metal analysis.

*2.5.2.1. Statistical analysis.* For simulation of the exposure-related accumulation of particles in the lung the following relationship was assumed: $dc/dt = a(1 - kt)$, where $k$ is the first-order elimination constant empirically determined during the postexposure period and $a$ is the daily increment of particle dose deposited in the alveoli. A dosimetric adjustment was made with regard to aerodynamic particle size (MMAD) using the Multiple-Path Particle Dosimetry Model (MPPD2) (Anjilvel and Asgharian, 1995; RIVM, 2002). The fate of inhaled particles was calculated based on elimination rate constants ($k = \ln(2)/t_{1/2}$ [days$^{-1}$]) of the lung particle burdens. Simulations were based using a respiratory minute volume of 1 l/min/kg-rat. This respiratory minute volume has been determined under conditions similar to this study (Pauluhn and Thiel, 2007). During exposure days, a fraction of the dose increment was added to each of the arrays, and the total accumulated lung dose was then calculated by the equation shown above over

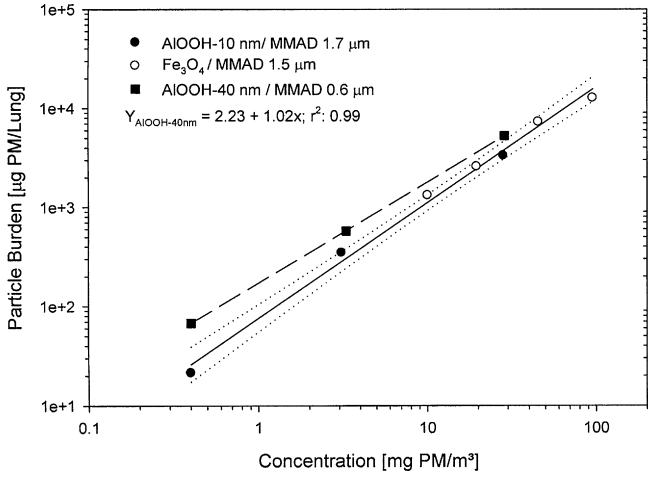


**Fig. 1.** Association of actual inhalation chamber concentrations of particulate matter and particle lung burden at the end of the 4-week exposure period based on the analysis depicted in Fig. 3. Aluminum oxyhydroxide (AlOOH) consisted of 10 and 40 nm primary nanocrystals with MMADs (agglomerated particles in inhalation chambers) of 1.7 and 0.6 μm, respectively. $Fe_3O_4$ consisted of 300–600 nm primary nanocrystals with an MMAD of 1.5 μm. Dotted lines represent the 95% confidence interval.

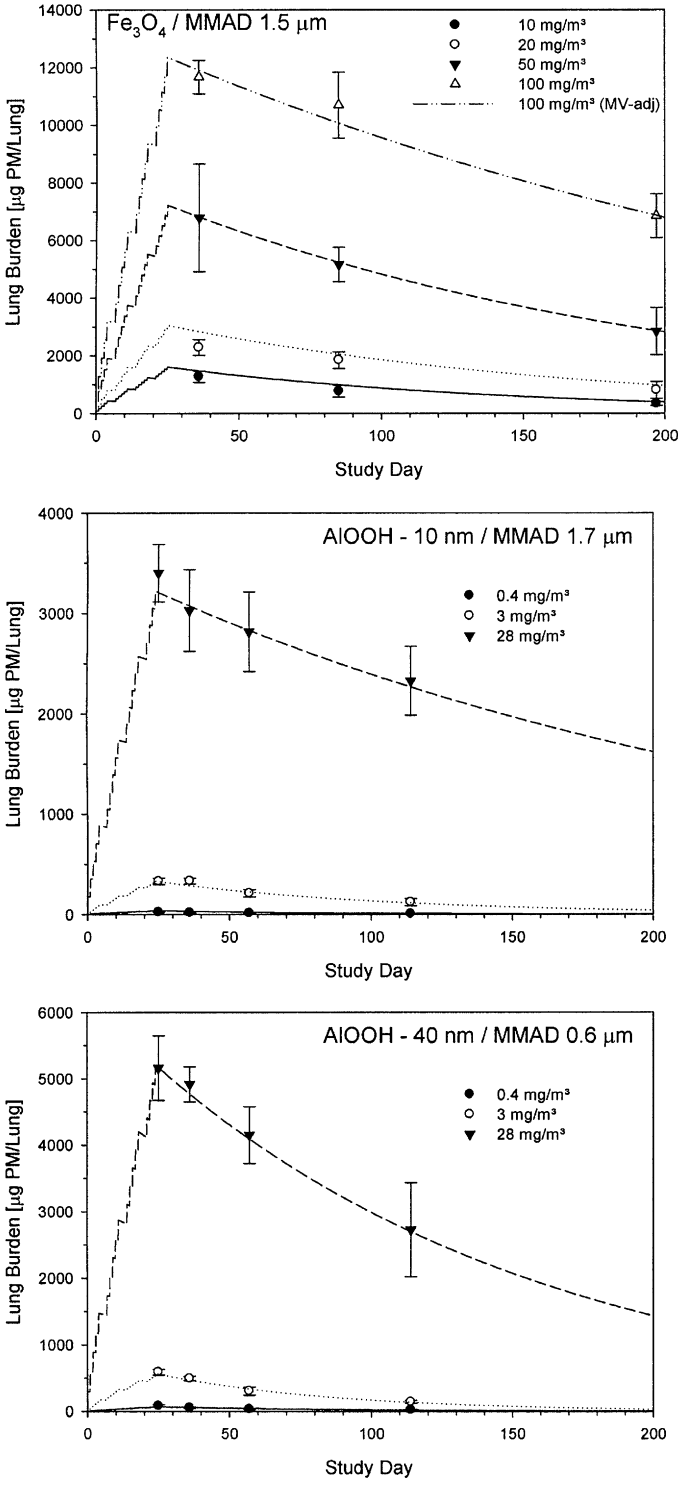


**Fig. 2.** Comparison of simulated and empirical relationships of particles retained in lungs from rats exposed for 4 weeks (6 h/day, 5 days/week) to fine $Fe_3O_4$ and AlOOH-10 nm and AlOOH-40 nm primary nanocrystals. Calculations took into account the different respirability of particles by using MPPD2 software. For rats exposed to 100 mg $Fe_3O_4$/m$^3$ respiratory minute volumes were adjusted from 1 to 0.85 l/kg-min due to assumed sensory irritation of dust. Empirical data points represent means ± S.D., six male rats per interim sacrifice.

the entire exposure period by superposition of the arrays. A Fortran computer code was used for calculations. BAL and organ weight data were compared by a one-way ANOVA and a Tukey–Kramer post hoc test. The criterion for statistical significance was set at $P<0.05$. Asterisks in figures and tables denote statistically significant differences to the concurrent air control group, $^{*}P<0.05$ and $^{**}P<0.01$.

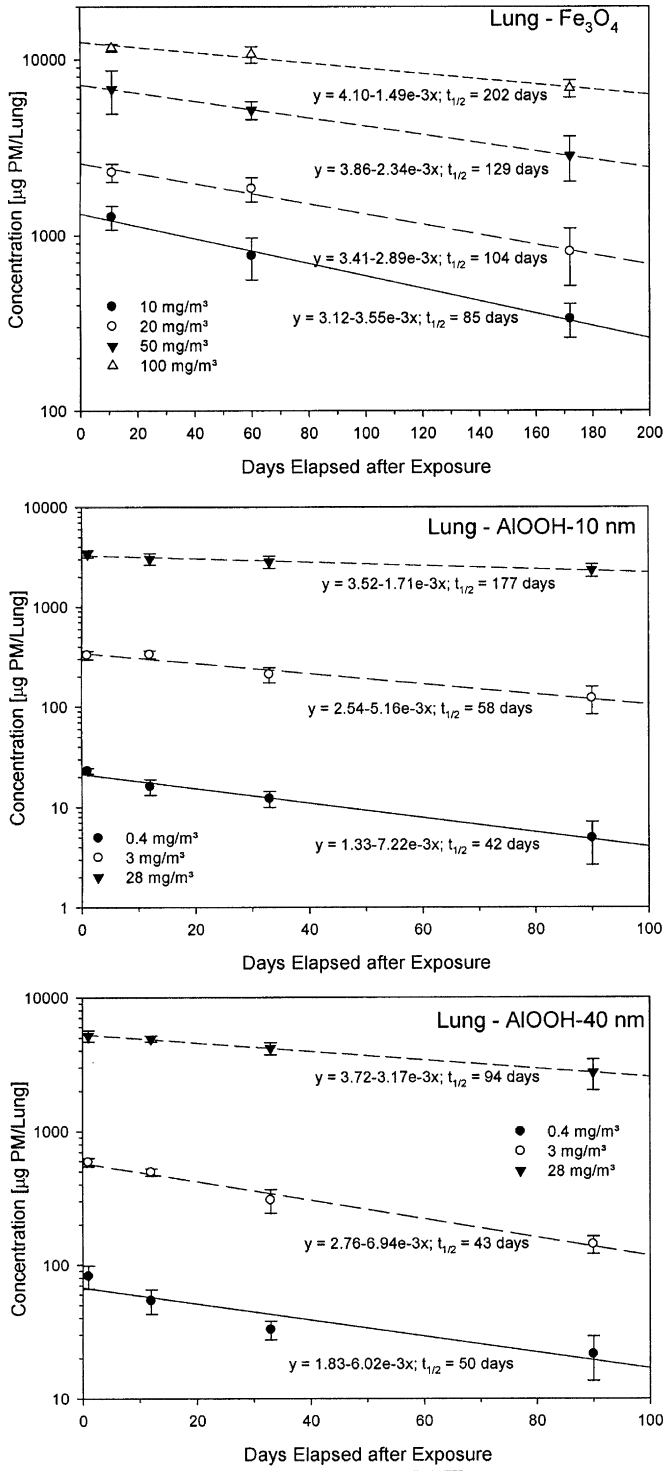


**Fig. 3.** Time-course and concentration-response analyses of particle mass in lungs from rats exposed for 4 weeks (6 h/day, 5 days/week) to fine $Fe_3O_4$ and AlOOH-10 nm and AlOOH-40 nm primary nanocrystals. Data points represent the means ± S.D. of six male rats per time point and group.

## 3. Results

### 3.1. Exposure atmosphere characterization

In the AlOOH-40 nm, AlOOH-10 nm, and $Fe_3O_4$ exposure groups, the average MMAD (GSD) was ≈0.6 µm (2.6), ≈1.7 µm (2.7), and ≈1.5 µm (2.1), respectively. The total mass concentrations from cascade impactor analyses were essentially similar to filter analyses. The mean (±S.D.) exposure concentrations were as follows: AlOOH-40 nm: 0.4 ± 0.11, 3.3 ± 0.55, and 28.7 ± 3.2 mg/m³; AlOOH-10 nm, 0.4 ± 0.06, 3.1 ± 0.32, and 28.3 ± 3.3 mg/m³; and $Fe_3O_4$: 10.1 ± 1.44, 19.7 ± 3.27, 45.61 ± 6.77, and 95.84 ± 17.6 mg/m³ (concentration > 1 mg/m³: 60 samples in total; at lower concentrations 17 samples in total were collected from inhalation chambers).

### 3.2. Pulmonary disposition

Rats were nose-only exposed to targeted particle concentrations bracketing a range from 0.4 to 96 mg/m³. Independent of the type of particle, the resultant cumulative particle lung burden was fairly proportional to the external, actual exposure concentration (Fig. 1). The highest lung burden relative to the exposure concentration occurred following exposure to AlOOH-40 nm/MMAD 0.6 µm. Exposure concentrations exceeding ≈10 mg PM/m³ resulted in lung burdens in the range of ≥1 mg PM/g lung (Fig. 1). When this lung burden was attained late during the 4-week exposure period (Fig. 2), the retention half-times were still in the normal range of $t_{1/2}$ = 60–70 days (Fig. 3). To the contrary, a precipitous increase in retention half-times occurred when exposure concentrations were in the range of above 30 mg PM/m³ (Figs. 2 and 3).

The simulated time-course of the cumulative pulmonary dose of AlOOH and $Fe_3O_4$ PMs, adjusted for pulmonary deposition using the MPPD2 model, matched the empirical data reasonably well at 3 and 28 mg/m³. However, at 0.4 mg/m³ AlOOH-10 nm simulated data were slightly over-predicted, whilst the respective data from AlOOH-40 nm matched the prediction (for details see Pauluhn, 2009). Due to PM-induced sensory irritation-related depression in ventilation observed in previous studies (kaolin, see Pauluhn, 2008), the respiratory minute volume of rats exposed to 100 mg $Fe_3O_4$/m³ was reduced by 15%.

Increased lung burdens of iron oxide and AlOOH-40 nm (MMADs 1.5–1.7 µm) were clearly correlated with longer half-times; however, only when not corrected for the pulmonary increase of iron load occurring in the control due to lung growth. Opposite

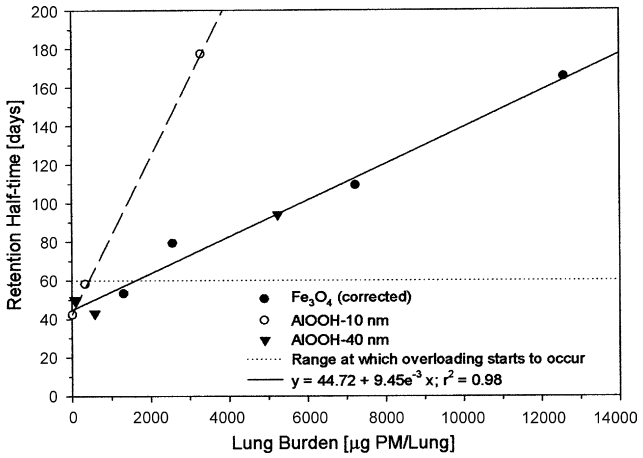


**Fig. 4.** Relationship of retention half-times and lung particle burdens from rats exposed for 4 weeks (6 h/day, 5 days/week) to fine $Fe_3O_4$ and AlOOH-10 nm and AlOOH-40 nm primary nanocrystals.

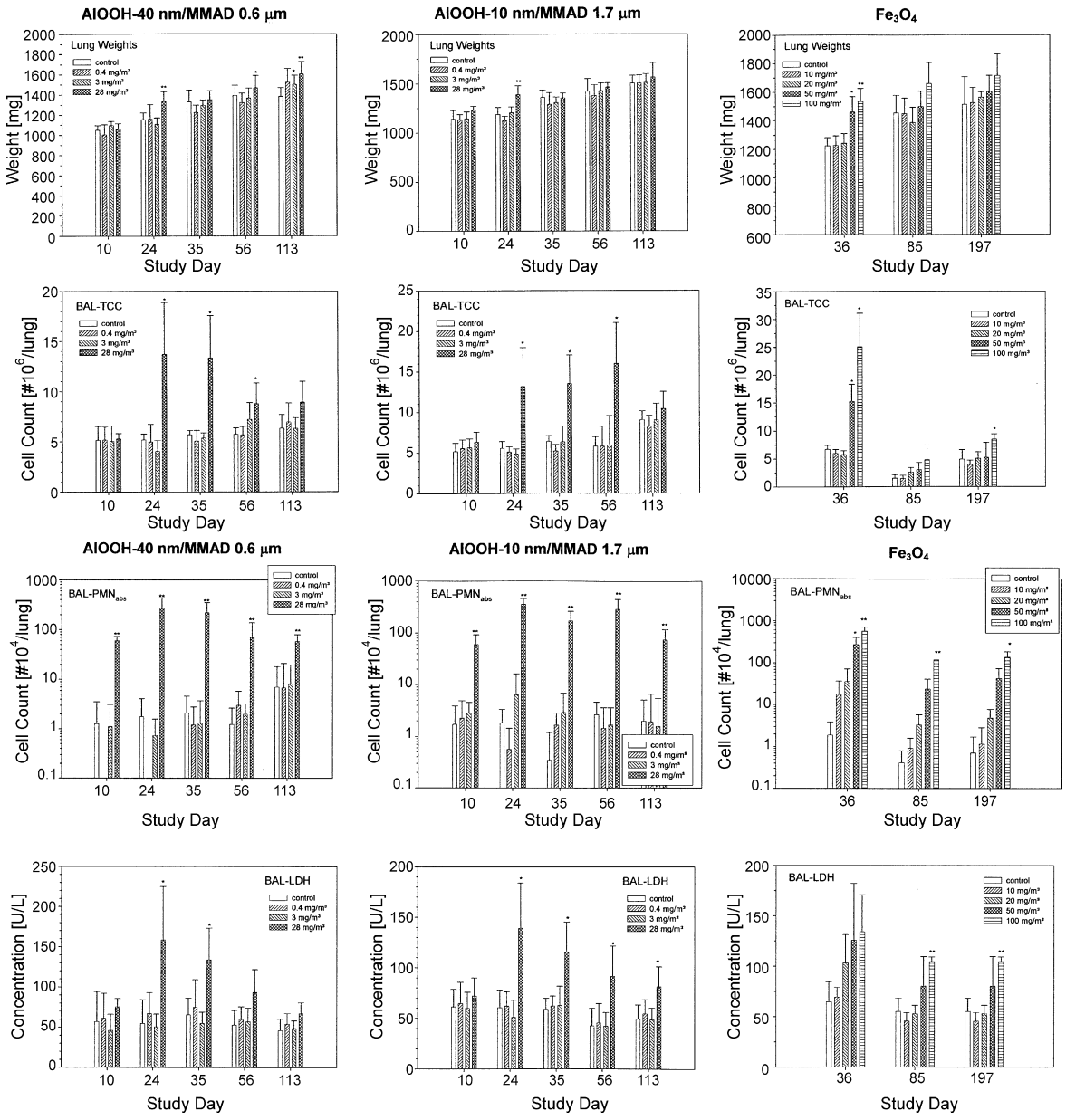


**Fig. 5.** Comparison of inflammatory endpoints in bronchoalveolar lavage fluid (BAL). Rats were exposed for 4 weeks (6 h/day, 5 days/week) to fine $Fe_3O_4$ and AlOOH-10 nm and AlOOH-40 nm primary nanocrystals. Data points represent the means ± S.D. of six male rats per time point and group. Asterisks denote statistical significance to the time-matched control ($^{*}P < 0.05$, $^{**}P < 0.01$).

to the half-times shown in Fig. 3, the respective corrected half-times were 53, 79, 109 and 165 days. The decrease in clearance was more pronounced for AlOOH-10 nm (MMAD 1.7 μm) as compared to AlOOH-40 nm (MMAD 0.6 μm) or $Fe_3O_4$ (MMAD 1.5 μm) (Fig. 4).

### 3.3. Bronchoalveolar lavage and lung weights

Details of findings in BAL from AlOOH studies have been detailed elsewhere (Pauluhn, 2009). Following exposure to AlOOH significant differences to the time-matched control occurred at 28 mg/m$^3$ only and changes were characterized by increased lung weights, LDH, protein, total cell counts (TCC), and neutrophilic granulocytes (PMNs). Key findings from the 4-week $Fe_3O_4$ study (sacrifice approximately 1 week postexposure) are included in Fig. 5. Similar changes occurred at 50 mg $Fe_3O_4$/m$^3$ and above. Somewhat equivocal changes of LDH and protein were observed on the first but not at subsequent postexposure sacrifices.

### 3.4. Comparison of key BAL-endpoints with PM-mass, -surface area, and -lung burden

Total cell counts, relative and absolute PMNs were compared relative to the actual exposure concentration, surface area (BET surface area × actual exposure concentration) and lung PM burden. The best correlations were obtained for mass-based exposure indices (Figs. 6–8) whereas the surface area provided the poorest correlation. In regard to absolute and relative PMNs, the correlation was always higher based on relative PMN counts. For all endpoints, the point of departure was attained at lung burdens of ≈1 mg/lung. Based on this metric, PM-specific differences in pulmonary inflammogenicity were not observed.

## 4. Discussion

Three independent essentially identically designed 4-week nose-only rat inhalation studies (exposure 6 h/day, 5 days/week) with ultrafine and fine poorly soluble particles were retrospectively compared to identify unifying denominators of pulmonary toxicity and exposure intensity. The test substances compared fulfil the criterion 'poorly soluble' and include synthetic black iron oxide ($Fe_3O_4$), which contains the transition element iron known to have variable oxidation states and thus be capable of redox-cycling, and aluminium oxyhydroxide (AlOOH) which has a stable oxidation state. Agglomerated AlOOH consisted of nanoparticles in the 10–40 nm range and was tested at MMADs of 1.7 μm (AlOOH-10 nm) and 0.6 μm (AlOOH-40 nm). The MMAD of fine $Fe_3O_4$ particles was similar to that of AlOOH-10 nm. Within each study concentration-dependent changes in particle size did not occur.

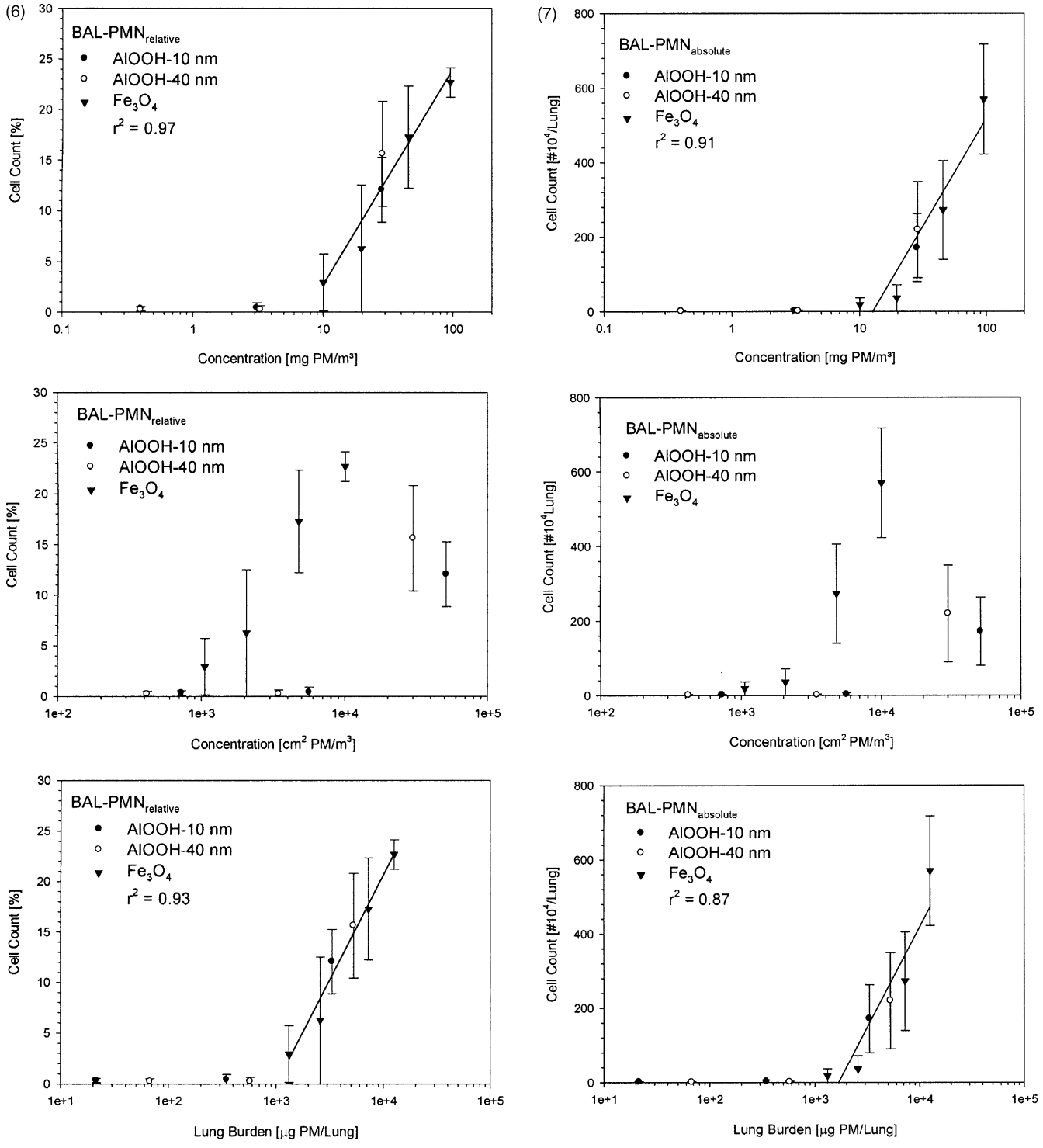


**Figs. 6–8.** Comparison of key inflammatory endpoints in bronchoalveolar lavage (TCC: total cell count, PMN: neutrophilic granulocytes, absolute or relative counts) with three exposure metrics—upper panel: mass-based actual exposure concentration; middle panel: surface area concentration (mass-based actual exposure concentration × BET surface area); lower panel: mass-based lung burden.

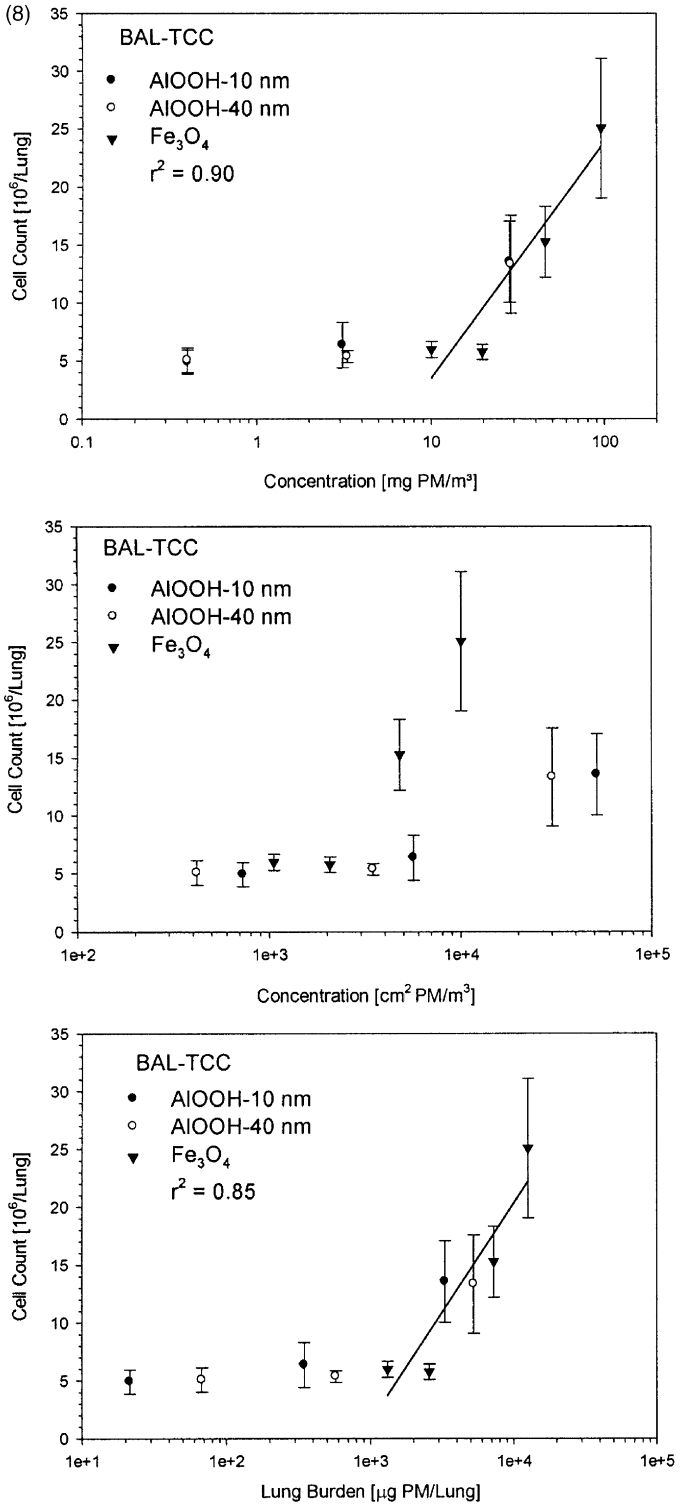


**Figs. 6–8.** (*Continued*).

This comparison demonstrates that determinations of target organ doses (lung) are most apt to integrate the particle mass deposited and retained in the lung. Hence, it is the most precise reflection of the cumulative inhaled dose and integrating multiple variables, such as the time-weighted daily exposure concentration, the respiratory minute volume, the aerodynamic size-dependent deposition efficiency, solubility, and resultant fate of retained particles. The cumulative lung burdens at the end of the 4-week period estimated from Fig. 3 demonstrate that the agglomerated particle size (MMAD) impacts the total lung burden to a greater extent than the size of primary particles (Fig. 1). Thus, lung burdens appear to be more dependent on the MMAD of agglomerated airborne particles, which determine the site of initial deposition within the respiratory tract, than on the size of primary particles. The latter appears to affect primarily the retention kinetics as shown for high lung burdens of AlOOH-10 nm. The elimination half-time of this substance was markedly higher when compared with AlOOH-40 nm and fine $Fe_3O_4$. This is consistent with published evidence show-

ing that primary particle size affected clearance kinetics (Bermudez et al., 2002, 2004; Brown et al., 2005). These findings support the supposition that nanosized particles (in the range of 10 nm) may disaggregate following deposition in the lung. Collectively, these results demonstrate that experimental approaches should address and differentiate deposition- and retention-related PM-induced effects. Suffice it to say, study protocols must allow for exposure and postexposure periods long enough to determine the time-course of particle loading and clearance, covering a cumulative range of lung burdens from non-overload to overload, to better understand whether pulmonary toxicity is clearly dependent on lung overload or is particle property-specific.

The elimination half-time for alveolar clearance in the non-overloading state (rats) has been reported to be in the range of 50–65 days (Donaldson et al., 2008; Stöber and McClellan, 1997; Brown et al., 2005). This evidence is consistent with this analysis, namely that lung burdens up to ≈1 mg PM/lung resulted in retention half-times in the range of 60 days and below (Fig. 4). For all three PMs the predicted, cumulative lung burdens matched reasonably well the actually observed lung burdens (Fig. 2). Simulations utilized published algorithms for particle deposition (MPPD2) and toxicokinetic constrains typical for poorly soluble, non-redox active PMs. Accordingly, lung burdens appear to be primarily determined by particle properties rather than dissolved/leached metal ions bound to tissue proteins.

With regard to BAL-PMNs the presentation of data relates either to "absolute" or "relative" counts which are used as such interchangeably in the published literature. Absolute counts take into account the total number of cells retrieved by BAL multiplied by the relative percentage obtained by cell cytodifferentiation. In this context, the terminology 'absolute PMN counts' appears to be somewhat inappropriate as the yield of cells harvested by BAL is much lower than the actual population of mobile cell types present in the alveoli and airways. In a previous study with AlOOH it was shown that approximately 20% of the particle lung dose was found in BAL-cells while that the remaining 80% of particle dose was likely in alveolar cells not accessible by the BAL procedures applied (Pauluhn, 2009). The comparison made in Figs. 6 and 7 shows a better correlation of $PMN_{relative}$ as compared to $PMN_{absolute}$. This supports the conclusion that preference should be given to data evaluations based on the actual results from cytodifferentiation which means percentages of PMNs ($PMN_{relative}$). The point of departure of endpoints in BAL suggestive of pulmonary inflammation matched the ≈1 mg PM/lung threshold at which lung overload starts to occur (Figs. 6–8; for lung weights see Fig. 5). Hence, the dispositional and toxicological findings are consistent with the common view held, namely that PM-related pulmonary toxicity is contingent upon the cumulative lung dose that exceeds overload conditions.

For pigment-grade synthetic $Fe_3O_4$ postexposure periods as long as 6 months were applied to study the fate (Figs. 2 and 3) and pulmonary toxicity (Fig. 5) of this potentially redox-active PM. As illustrated in Figs. 1 and 2, the cumulative lung burdens of non-calcined, crystallized iron oxide was consistent with that of calcined AlOOH-40 nm. Accounting for differences in deposition efficiencies by using actual PM lung burdens, for all particles compared a unifying target organ dose–response relationship could be established (Figs. 6–8). This coincidence appears to provide supportive evidence that facilitated dissolution of $Fe_3O_4$ particles does not take place to any appreciable extent or that these particles have any superimposed inflammogenicity due to other than PM-related mechanisms. Results from inhalation studies with calcined red iron oxide ($Fe_2O_3$, haematite) support this conclusion (Pauluhn, unpublished data).

It is generally conceived that the conceptually better alternative to particle mass or number as a measure of dose would be the surface area/activity. Surface area rather than mass accounts for the fact that biopersistent particles can interact only by contact of their surface, determining an effective dose rate by a catalytic surface reaction rate that accumulates to an effective dose with increasing residence time in the target tissue (Stöber and McClellan, 1997). Along with these concerns and the risks exposure to nanomaterials may pose to workers, issues regarding the most appropriate unifying metric of dose are still unresolved (Maynard, 2007). This issue is complicated further as the surface area using the BET methodology *per se* is not necessarily a unique characteristic of a particle. The BET (Brunauer, Emmett, and Teller) theory is a rule for the physical adsorption of gas molecules on a solid surface and serves as the basis for an important analysis technique for the measurement of the specific surface area of a material (Brunauer et al., 1938). Methodological differences in the pre-conditioning of particles or measurement may also result in different binding isotherms of $N_2$. For instance, the specific surface area ($N_2$ used as adsorbent) of AlOOH-40 nm, after drying and degassing (100 °C at 0.1 mbar for 16 h) was 46.3 $m^2/g$ while under other conditions of measurement (550 °C for 3 h) the BET was reported to be 105 $m^2/g$. Actually available binding sites of key proteins or peptides on particles and competitive factors present in the alveolar lining fluids are yet incompletely elucidated. Therefore, surface area *per se* may be an incomplete reflection of the potentially 'biologically active' critical surface area. Thus, the 'biologically active' surface area may vary from one circumstance to another.

Optimally, the choice of dose metric and normalizing factors should be based on the biological mechanisms mediating the toxic outcome. The analysis made in Figs. 6–8 clearly demonstrates that the mass-based cumulative lung burden is a substantially better metric than surface area, suggesting toxicity is mediated via activated inflammatory cells rather than via particle properties. The mass-based (actual concentration × cumulative exposure duration) exposure intensity appears to be also suitable; however, aerodynamic particle size related changes in pulmonary deposition have to be accounted for.

In summary, this analysis provides strong evidence that the cumulative lung exposure dose corresponded well with the mass-based and agglomerated particle size-adjusted external exposure concentration and the associated pulmonary inflammatory response. The inhalation study with a MMAD in the range of ≈0.5 μm yielded a higher pulmonary dose than MMADs in the 1–2 μm range. In regard to the human significance of rat inhalation bioassays with poorly soluble particles, their outcome is highly contingent upon the total lung burden and especially whether overloading or non-overloading conditions had been attained. These conclusions are coherent with published evidence (International Life Science Institute (ILSI), 2000). Hence, a key premise for the dosimetric adjustment across species is that comparable lung tissue doses should cause comparable effects. From that perspective, the determination of mass-based pulmonary lung burdens appears to be amongst the most important and critical nominator of dose.

## Conflict of interest

None.

## Acknowledgments

The previously published studies with aluminum oxyhydroxides (Pauluhn, 2009) were funded by the German BMBF-NanoCare Project (BMBF: German Federal Ministry of Education and Research). The iron oxide study was sponsored by a consortium of twelve European Iron Oxide producers/importers.

## References


Anjilvel, S., Asgharian, B., 1995. A multiple-path model of particle deposition in the rat lung. Fundam. Appl. Toxicol. 28, 41–50.

Bacon, B.R., Britton, R.S., 1990. The pathology of hepatic iron overload: a free radical-mediated process? Hematology 11, 127–137.

Bermudez, E., Mangum, J.B., Asgharian, B., Wong, B.A., Revery, E.E., Janszen, D.B., Hext, P.M., Warheit, D.B., Everitt, J.I., 2002. Long-term pulmonary responses of three laboratory rodent species to subchronic inhalation of pigment-grade titanium dioxide particles. Toxicol. Sci. 70, 86–97.

Bermudez, E., Mangum, J.B., Wong, B.A., Asgharian, B., Hext, P.M., Warheit, D.B., Everitt, J.I., 2004. Pulmonary responses of mice, rats, and hamsters to subchronic inhalation of ultrafine titanium dioxide particles. Toxicol. Sci. 77, 347–357.

Brain, J.D., Frank, N.R., 1968a. The relation of age to the numbers of lung free cells, lung weight, and body weight in rats. J. Gerontol. 23, 58–62.

Brain, J.D., Frank, N.R., 1968b. Recovery of free cells from rat lungs by repeated washings. J. Appl. Physiol. 25, 63–69.

Brown, J.S., Wilson, W.E., Grant, L.D., 2005. Dosimetric comparisons of particle deposition and retention in rats and humans. Inhal. Toxicol. 17, 355–385.

Brunauer, S., Emmet, P.H., Teller, E., 1938. Adsorption of gases in multimolecular layers. J. Am. Chem. Soc. 60, 309–318.

Directive 86/609/EEC, 1986. Guideline of the council dated November 24, 1986 on the reconciliation of legal and administrative regulations of the member countries for the protection of animals used for studies and other scientific purposes. J. Eur. Community 29, 1–28 (Legal Specifications L358).

Donaldson, K., Borm, P.J.A., Oberdorster, G., Pinkerton, K.E., Stone, V., Tran, C.L., 2008. Concordance between in vitro and in vivo dosimetry in the proinflammatory effects of low-toxicity, low-solubility particles: the key role of the proximal alveolar region. Inhal. Toxicol. 20, 53–62.

Ferin, J., Oberdorster, G., Penny, D., 1992. Pulmonary retention of ultrafine and fine particles in rats. Am. J. Respir. Cell Mol. Biol. 6, 535–542.

Fubini, B., Mollo, L., Giamello, E., 1995. Free radical generation at the solid/liquid interface in iron containing minerals. Free Radic. Res. 23, 593–614.

International Life Science Institute (ILSI), 2000. The relevance of the rat lung response to particle overload for human risk assessment: a workshop consensus report—ILSI risk science institute workshop participants. Inhal. Toxocol. 12, 1–17.

Maynard, A.D., 2007. Nanotechnology: the next big thing, or much ado about nothing? Ann. Occup. Hyg. 51, 1–12.

Monteiller, C., Tran, L., MacNee, W., Faux, S., Jones, A., Miller, B., Donaldson, K., 2007. The pro-inflammatory effect of low-toxicity low-solubility particles, nanoparticles and fine particles, on epithelial cells in vitro; the role of surface area. Occup. Environ. Med. 64, 609–615.

Morrow, P.E., 1988. Possible mechanisms to explain dust overloading of the lungs. Fundam. Appl. Toxicol. 10, 369–384.

Morrow, P.E., 1992. Dust overloading in the lungs. Toxicol. Appl. Toxicol. 113, 1–12.

National Institute for Public Health and the Environment (RIVM), 2002. Multiple Path Particle Dosimetry Model (MPPD2 v. 1.0): A Model for Human and Rat Airway Particle Dosimetry. RIVA Report 650010030, Bilthoven, The Netherlands.

Oberdörster, G., Ferin, J., Morrow, P.E., 1992. Volumetric loading of alveolar macrophages (AM): a possible basis for diminished AM-mediated particle clearance. Exp. Lung Res. 18, 87–104.

Pauluhn, J., 2005. Retrospective analysis of acute inhalation toxicity studies: comparison of actual concentrations obtained by filter and cascade impactor analyses. Regul. Toxicol. Pharmacol. 42, 236–244.

Pauluhn, J., Thiel, A., 2007. A simple approach to validation of directed-flow nose-only inhalation chambers. J. Appl. Toxicol. 27, 160–167.

Pauluhn, J., 2008. Comparative assessment of early acute lung injury in mice and rats exposed to 1,6-hexamethylene diisocyanate-polyisocyanate aerosols. Toxicology 247, 33–45.

Pauluhn, J., 2009. Pulmonary toxicity and fate of agglomerated 10 and 40 nm aluminum oxyhydroxides following 4-week inhalation exposure of rats: toxic effects are determined by agglomerated, not primary particle size. Toxicol. Sci., in press.

Stöber, W., McClellan, R.O., 1997. Pulmonary retention and clearance of inhaled biopersistent aerosol particles: data-reducing interpolation models and models of physiologically based systems. A review of recent progress and remaining problems. Crit. Rev. Toxicol. 27, 539–598.

Ullmann's Encylclopedia of Industrial Chemistry, 1992. Pigments, Inorganic, vol. A20. VCH Verlagsgesellschaft, Weinheim, p. 303.

Warheit, D.B., Brock, W.J., Lee, K.P., Webb, T.R., Reed, K.L., 2005. Comparative pulmonary toxicity inhalation and instillation studies with different $TiO_2$ particle formulations: impact of surface treatment on particle toxicity. Toxicol. Sci. 88, 514–524.

Warheit, D.B., Webb, T.R., Reed, K.L., Frerichs, S., Sayes, C.M., 2007. Pulmonary toxicity study in rats with three forms of ultrafine. $TiO_2$-particles: differential responses related to surface properties. Toxicology 230, 90–104.

Warheit, B.D., 2008. How meaningful are the results of nanotoxicology studies in the absence of adequate material characterization? Toxicol. Sci. 101, 183–185.

Winterbourn, C.C., 1995. Toxicity of iron and hydrogen peroxide: the Fenton reaction. Toxicol. Lett. 82/83, 969–974.